

Magnetic Molecules at the Air/Water Interface

D. Vaknin,^{*,†} L. L. Miller,[†] M. Eshel,[‡] and A. Bino[‡]*Ames Laboratory and Department of Physics and Astronomy, Iowa State University, Ames, Iowa 50011, and Department of Inorganic and Analytical Chemistry, The Hebrew University of Jerusalem, 91904 Jerusalem, Israel**Received: March 22, 2001; In Final Form: June 8, 2001*

X-ray Reflectivity (XR) and grazing angles of incidence X-ray diffraction (GIXD) were conducted to determine the structure of $\text{Cr}_8\text{O}_4(\text{O}_2\text{CPh})_{16}$ Langmuir films at the air/water interface at various surface pressures π . The molecular area versus pressure, π - A isotherm, reflectivity, and GIXD variation (width and peak position) with compression, all imply the formation of a homogeneous monolayer at very low surface pressures. The film is disordered with a liquidlike or glassy structure factor at all pressures, with correlation lengths that extend over a few molecular distances. The liquidlike state of the monolayer and an incomplete formation of a second layer have implications on the quality of transferred Langmuir–Blodgett films.

Introduction

Magnetic molecules with strong intramolecular magnetic exchange interactions relative to intermolecular ones are of interest for both their unique fundamental magnetic properties and their potential technological applications.¹ Typically organometallic based, these “molecular magnets” consist of two or more 3d or 4f magnetic ions coupled by electronic superexchange interactions, and can be over 10 nm in size. The controllable size and geometries of the magnetic ions are of fundamental importance to testing our understanding of magnetic interactions and have already lead to the discovery of the quantum tunneling effect of the magnetic spins.² As the number of magnetic ions is increased, one approaches the mesoscopic regime which bridges the nanoscopic scale and the macroscopic world of extended lattice solids. On the basis of their small size and customization possibilities, the materials are potentially very high-density storage medium or functional building blocks in supramolecules. Some magnetic molecules occur naturally as biological materials which makes their study appealing to an even wider audience and gives added importance to their study.

Herein we present our structural study of a two-dimensional (2D) Langmuir film formed by the magnetic molecule $\text{Cr}_8\text{O}_4(\text{O}_2\text{CPh})_{16}$.^{3,4} The antiferromagnetic Cr_8O_4 cubane core, shown in Figure 1, is similar to the compound described by Atkinson et al.³ containing two coupling constants (J) -3 and -5 K. This molecule is readily soluble in CHCl_3 , and possesses a hydrophobic outer shell composed of 16 phenyl rings making it a potential monolayer former when spread on water surfaces. Such monolayers can be subsequently transferred to solid surfaces employing the Langmuir–Blodgett (LB) technique to form well-defined multilayer systems. Control of their arrangement on solid surfaces is an important step to potential applications of these molecular magnets in electronic or magnetic devices. Such control has to be achieved prior to the LB transfer while the molecules are spread as a Langmuir film at aqueous interfaces. The Langmuir trough readily allows for the manipulation of

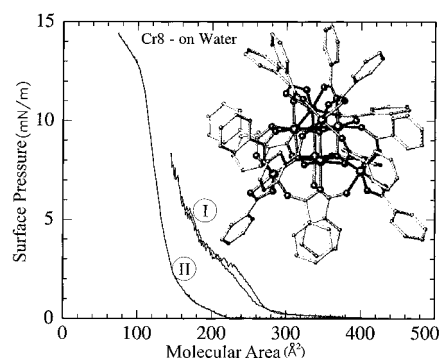


Figure 1. The Cr8 molecule [$\text{Cr}_8\text{O}_4(\text{O}_2\text{CPh})_{16}$] used in this study, and surface pressure versus molecular-area (π - A) isotherm of Cr8 on pure water. Two sets of π - A isotherms (at $T = 20$ °C) taken at compression rates 4 (curves labeled I) and 30 (II) per molecule per minute are shown. The isotherm was found to be sensitive to the compression rate; however, for compression rates that are slower than approximately 10 \AA^2 per molecule per minute, the isotherms are similar to curve I. The slow rate isotherm indicate that the molecules interact at relatively large molecular areas, around $300\text{--}350 \text{ \AA}^2$ (we estimate the cross section of the molecule at 232 \AA^2). It is argued that the fast compression rate does not allow for the formation of a single layer, driving the system into a multilayer form. All X-ray experiments were performed on slow-rate compressed samples.

the film by the variations of the in-plane density, pH, ionic concentration, and temperature of the subphase. In addition, desired separation among magnetic molecules can be achieved by spreading them from a mixture that includes fatty acids or lipids (assuming that they are miscible among acyl chains) that can provide a supporting 2D membrane to the embedded magnetic molecules. Similar attempts to form LB films of organometallic Mn12-acetate compound were reported recently.⁵ In those studies the Mn12 molecule was embedded in multilayer fatty acid (behenic acid) where the Mn12 formed an intercalated layer between the two headgroups of adjacent fatty acids.⁶

More generally, the Cr8 molecule can serve as a model system to study the 2D physical properties of highly symmetric molecules that reside on an isotropic substrate, i.e., aqueous surfaces. A similar motivation to understand the effects of physical dimension on statistical physics, led to recent studies

* To whom correspondence should be addressed. E-mail: vaknin@ameslab.gov.

[†] Ames Laboratory and Department of Physics and Astronomy.

[‡] Department of Inorganic and Analytical Chemistry.

of C60-propylamine adduct monolayers at the air/water interface.⁷ We have undertaken this study to examine the feasibility of forming a single homogeneous layer of Cr8 on water.

Experimental Details

The $\text{Cr}_8\text{O}_4(\text{O}_2\text{CPh})_{16}$ compound was prepared according to the method described in the literature^{3,4} and the use of acetonitrile for crystallization. Samples were weighed directly into volumetric flasks and were subsequently filled with chloroform (HPLC grade, Fisher Scientific, Fair Lawn, NJ) to form homogeneous bluish solution. Langmuir monolayers were prepared on pure water (Milli-Q apparatus Millipore Corp., Bedford, MA; resistivity, 18.2 M Ωcm) in a temperature-controlled Teflon trough maintained at 18–20 °C in a gastight aluminum container. Surface-pressure was measured with a microbalance using a filter-paper Wilhelmy plate. To reduce incoherent scattering from air, and to slow film deterioration by oxidation due to production of radicals by the intense synchrotron beam, the monolayer was kept under a He environment during the X-ray measurements. No noticeable differences were found in the π - A isotherms when performed under air or He environments.

In-situ X-ray reflectivity experiments from films, spread at the air-water interface, were carried out on a liquid-surface reflectometer at Ames Laboratory using the $\text{CuK}\alpha$ radiation of a rotating anode (Rigaku, UltraX 18). The GIXD experiments were carried out on the newly built Liquid Surfaces Diffractometer on the 6ID-B beamline at the Advanced Photon Source at Argonne National Laboratory. A downstream Si double crystal monochromator selects the X-ray beam at the desired energy ($\lambda = 1.5498 \text{ \AA}$). The highly monochromatic beam is deflected onto the liquid surface to the desired angle of incidence with Ge(111) crystal. For each angle of incidence, the θ_M and $2\theta_M$ angles of the Ge(111) crystal and diffractometer are adjusted.

Results and Discussion

Figure 1 shows two sets of surface-pressure versus molecular area (π - A) isotherms for Cr8 at $T = 20 \text{ C}$; taken at compression rates 4 (curves labeled I) and 30 (II) \AA^2 per molecule per minute. As shown, the isotherm was found to be sensitive to the compression rate. However, compressions at rates slower than approximately 10 \AA^2 per molecule per minute yielded isotherms similar to curve I. The slow rate isotherm indicated that the molecules interact at relatively large molecular areas (300–350 \AA^2), compared to the estimated cross section of the molecule at 250 \AA^2 . Decompression and subsequent compression of the film yielded π - A isotherms with onsets for abrupt increase in pressure at molecular area that is smaller than the one before decompression. This behavior can be due to the formation of a second layer or to a loss of molecules into the subphase. Our reflectivity and GIXD experiments suggest that the formation of multiple layers occurs in the compression-decompression process. The compression-decompression cycle indicates that the film does not expand significantly in the decompression process, but actually breaks apart to large domains, which are held together by the relatively strong intermolecular forces (compared to their interaction with water). We argue that, at very low surface pressures, above about 0.1 mN/m and below $\sim 5 \text{ mN/m}$, the molecules form an intact monolayer, due to the strong attractive interactions among neighboring molecules. However the monolayer can be inhomogeneous with patches of uncovered water, as demonstrated by the GIXD. All X-ray scattering experiments were conducted on samples that were

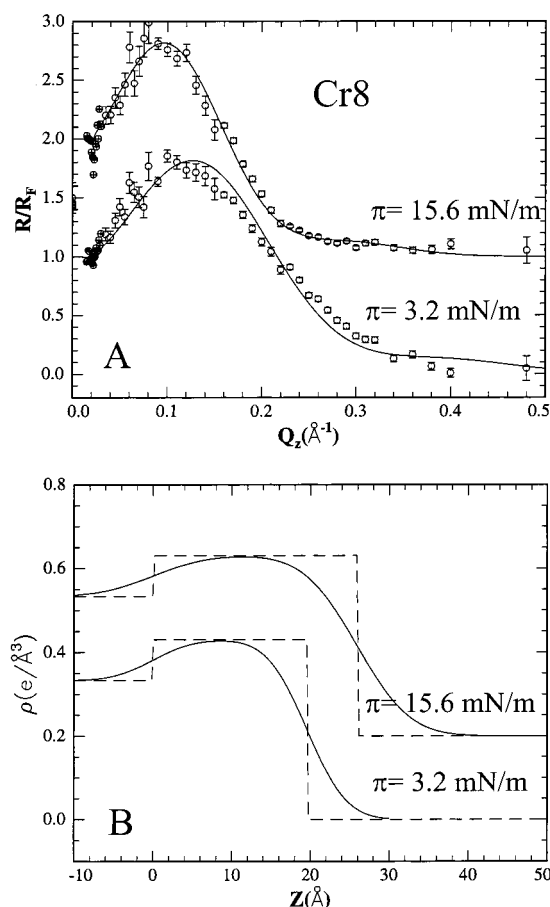


Figure 2. Measured reflectivity curves versus momentum transfer Q_z (normalized to pure subphase reflectivity R_F ; performed on the rotating anode at Ames Laboratory) (A). The solid lines are the best fit to the reflectivity data using a standard one-slab electron density model as shown in (B). Whereas the film consists of a single layer below $\sim 5 \text{ mN/m}$, the thickness of the film at $\pi = 15.6 \text{ mN/m}$ suggests the formation of a second layer at high surface pressures. The rod scans at the 2D Bragg reflection indicate that the second layer is completely disordered.

compressed at the slow rate, 4 \AA^2 per molecule per minute (as in curve I of Figure 1). Once the monolayer was compressed to a certain surface pressure, it was found to be very stable over the course of the X-ray scattering experiments (6–12 h), and therefore did not require any adjustments.

Specular XR experiments were conducted to determine the electron densities across the interface and to relate them to molecular arrangements in the film. Figure 1A shows reflectivity curves normalized to the calculated reflectivity of ideally flat water interface, R_F versus the momentum transfer Q_z at different pressures (obtained with the rotating anode X-ray source). To extract the electron density profile across the interface, the data was fitted to a calculated reflectivity as follows

$$R(Q_z) = R_0(Q_z)e^{-(Q_z\sigma)^2} \quad (1)$$

where $R_0(Q_z)$ is the reflectivity from steplike functions (representing the slab model $\rho(z)$) calculated by the recursive dynamical method,⁸ and σ is an effective surface roughness associated with the Debye-Waller-like term $e^{-(Q_z\sigma)^2}$. The model electron density across the interface $\rho(z)$ consisted of a single slab, with three varied parameters: the thickness of the slab, its electron density, and its surface roughness. Figure 2A shows fits to the data (solid lines) using the corresponding electron densities shown in Figure 2B. The reflectivity at low pressures

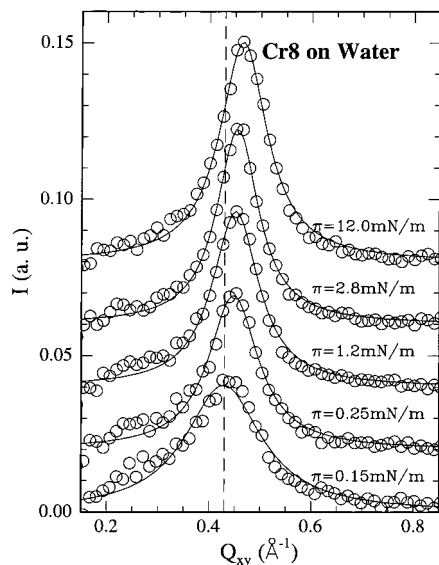


Figure 3. GIXD scans from Cr8 monolayer at various points of the π - A isotherm. The width of the Bragg peak indicates short-range 2D order. The peak corresponds to a d spacing 14.9 Å which when compared to the molecular diameter 17–18 Å, implying 2D hexagonal packing.

(below ~ 5 mN/m) yields a film thickness of approximately 17–19 Å, consistent with the estimated largest diameter of the molecule ($R \approx 17$ –18 Å), indicating the formation of a single layer at the interface. At higher pressures the thickness of the film, as extracted from the reflectivity, indicates the formation of a second layer.

Using the electron density and A_{GIXD} (the molecular area determined from the GIXD), the total number of electrons per average in-plane unit cell can be estimated as follows:

$$N_{\text{Ref}} = A_{\text{GIXD}} \int \rho(z) dz \quad (2)$$

yielding $N_{\text{Ref}} = 1880 \pm 200$ electrons per average unit cell at $\pi = 3.2$ mN/m, whereas the actual number of electrons per molecule is $N = 1232$. Such a discrepancy can be due to the contribution of integrated water molecules in the film (approximately 65 water molecules per Cr8) in particular, in the void between phenyl groups and close to the hydrophilic CrO core. Another explanation to this difference in the number of electrons can be that it is due to a partial formation of a second layer. Both, a hydration sphere around the molecule, and incomplete secondary layer have significant implications regarding the deposition of more than one layer of this molecule during a LB process.

To determine the lateral organization of the film GIXD were conducted at various points along the isotherm. In these experiments, the angle of the incident beam with respect to the surface is fixed below the critical angle for total reflection. Figure 3 shows diffraction patterns from the monolayer at various points along the isotherm. At finite pressures, GIXD scans in the range $0.05 \leq Q \leq 2.0 \text{ \AA}^{-1}$ revealed a prominent peak centered at $Q_{xy} \approx 0.428$ – 0.465 \AA^{-1} with a full width at half-maximum (fwhm) that is much broader than the resolution of the diffractometer ($\sim 0.01 \text{ \AA}^{-1}$) characteristic of short-range order (SRO). For a molecular area $A_{\text{iso}} = 265 \text{ \AA}^2$ (extracted from curve I isotherm, $\pi \approx 0.3$ mN/m) the peak position center at $Q_{xy}^0 \approx 0.428 \text{ \AA}^{-1}$ corresponds to a d spacing $2\pi/Q_{xy}^0 \approx 14.9 \text{ \AA}$, which is slightly smaller than the estimated molecular diameter. The observation of a single Bragg peak in the diffraction pattern suggests that SRO is either of hexagonal or

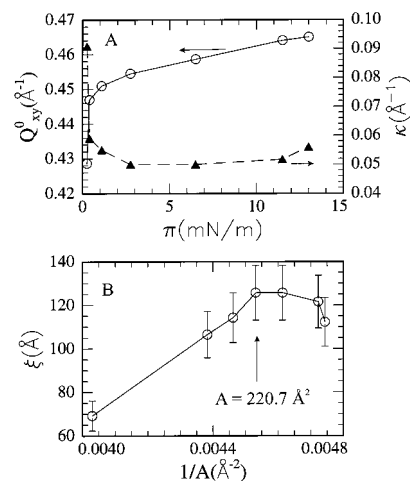


Figure 4. (A) Peak position, and line width κ as determined from the GIXD experiments as a function of the lateral pressure (B) Correlation length versus in-plane density of the molecules. The linear behavior regime is referred to as 2D liquidlike, whereas at molecular areas that are smaller than 220 \AA^2 (~ 5 mN/m) the system transforms to a glassy state. The small changes at high densities are ascribed to possible interdigitation among phenyl groups of neighboring molecules.

square symmetry. Assuming hexagonal or square SRO, correspond to an average nearest-neighbor distance $a_{\text{hex}} = 17.2 \text{ \AA}$ or $a_{\text{square}} = 14.9 \text{ \AA}$ and a molecular area $A_{\text{GIXD}} \approx 252 \text{ \AA}^2$ or $A_{\text{GIXD}} \approx 222 \text{ \AA}^2$, respectively. The diameter of the molecule that determines NN distance is governed by the largest edge-to-edge distance between phenyl groups $D \approx 17$ –18 Å, and therefore it is reasonable to conclude that the in-plane SRO is hexagonal. At very low pressures there is a small difference between A_{iso} (265 \AA^2 ; curve I in Figure 1) and A_{GIXD} (252 \AA^2). This difference and the broad line width can result from an incomplete coverage of the water surface. The variation of the line width indicates a 2D liquidlike system that can be described in terms of the Ornstein–Zernike structure factor for liquids with

$$I(Q_{xy}) \sim \frac{C}{1 + (\Delta Q_{xy}/\kappa)^2} \quad (3)$$

where C is a constant, κ is inversely proportional to the correlation length $\Delta Q_{xy} \equiv Q_{xy} - Q_{xy}^0$. Figure 4A shows the variation of peak position and κ as a function of the lateral pressure π , where an abrupt increase in the correlation length at low pressures is observed. Figure 4B shows the variation of the positional correlation length versus the inplane molecular density. The correlation length increases linearly with density increase, but it does not diverge as in systems that exhibit long-range-order. At this linear regime we argue that the 2D system behaves like a 2D liquid. At molecular areas that are smaller than $A_{\text{GIXD}} \approx 220 \text{ \AA}^2$, the correlation length reaches a maximum with a slight trend of falling off at higher densities. This increased disorder as the monolayer is compressed can be due to an irregular interdigitation among phenyl groups of neighboring molecules. At this density region the system is almost incompressible behaving like a glass. Similar GIXD results were reported for monolayers of C60-propylamine on water surfaces. In this case the outer shell of the fullerene adduct is hydrophobic due to the alkyl chains, and its core is hydrophilic due to amine headgroups that reside on the fullerene surface.⁹ GIXD and Brewster angle microscopy results demonstrated that C60-propylamine monolayers form a 2D amorphous solid,⁷ with a broad 2D Bragg reflection that was practically independent of

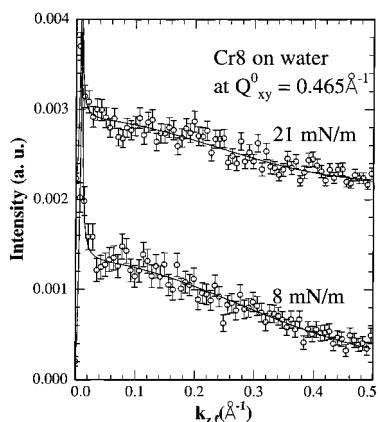


Figure 5. Intensity versus $k_{zf} \equiv k_0 \sin \beta$, where β is the angle of the scattered beam with respect to the water surface. These rod-scans were taken at the 2D Bragg peak Q_{xy}^0 . The solid line is a fit to the spherical structure factor given in eq 5 yielding a molecular diameter $R = 6\text{--}7$ Å even at high pressures. This shows that the second layer observed in the reflectivity experiments at high pressures (Figure 2), does not contribute to the Bragg reflection and therefore is completely disordered.

surface pressure. By contrast, the pronounced response of the Cr8 monolayers to the lateral pressure (peak position and width; see Figure 4) indicates that the 2D system is compressible and liquidlike to at least 5 mN/m.

Rod scans along the surface normal at the 2D Bragg reflection were conducted to determine the form factor of the diffracting objects and also to provide another measure for film thickness. This thickness can in principle be different than that measured by the reflectivity. The reflectivity is collected from the whole footprint of the incident beam on the surface (the illuminated area), averaging over a macroscopic portion of the sample. By contrast, the rod scan at the Bragg reflection probes the thickness of the diffracting ordered domains which can be microscopic in size. In these scans, the intensity versus k_{zf} ($\equiv k_0 \sin \beta$; where $k_0 = 2\pi/\lambda$, and β is the angle of the scattered beam with respect to the surface), is measured at the 2D Bragg reflection Q_{xy}^0 . Two such rod scans at $\pi = 4.2$ mN/m and at 8 mN/m are shown in Figure 5 (similar rod scans were observed at higher surface pressures). For an ideal 2D system the intensity along the rod is a constant except for an enhancement due to dynamical scattering at the critical angle for total reflection β_c . The fall off of the intensity shown in Figure 5 is consistent with the finite thickness of the film. Quantitatively, the intensity along the rod of the 2D Bragg reflection can be analyzed in the framework of the distorted wave Born approximation (DWBA) using^{10,11}

$$I \propto |t(k_{zf})|^2 |F(Q_z)|^2 \quad (4)$$

where $t(k_{zf})$ is the Fresnel transmission function which gives rise to the enhancement around the critical angle, as seen in Figure 5. Here, it is assumed that the molecule can be approximated by a homogeneous sphere of radius R with a structure factor

$$F(Q_z) = [\sin(Q_z R) - Q_z R \cos(Q_z R)] / (Q_z R)^3 \quad (5)$$

The solid lines in Figure 5 are the best fit to the data yielding a radius $R = 6.2 \pm 0.5$ Å at $\pi = 4.2$ mN/m, and $R = 6.7 \pm 0.5$

Å at $\pi = 8$ mN/m. This radius is larger than that of the CrO core of the molecule (≈ 3.0 Å) which has a higher electron density than the outer shell of the molecule that consists of phenyl groups ($R \approx 8.5\text{--}9$ Å). The value for R , which is extracted from the rod scan, represents an average effective radius of the electron density of a Cr8 molecule. At low pressures, this thickness together with the reflectivity show that the film consists of a single layer. However at surface pressures higher than ~ 5 mN/m the average film thickness extracted from the reflectivity is approximately twice that extracted from the rods. Whereas the reflectivity indicates the formation of a second layer, the rod scan analysis shows that the second layer does not contribute to the Bragg reflection observed. This suggests that the second layer is extremely disordered lacking even short-range order, due to the fact that the second layer is incomplete.

Conclusions

The π -A isotherm, X-ray reflectivity, and GIXD variations (width and peak position, and rod scan) with compression, all imply the formation of a monolayer at the air-water interface at surface pressures that are smaller than 3–5 mN/m. The monolayer is disordered with a liquidlike structure factor, and correlation-lengths that extend over a few molecular distances. The electron density profile extracted from the reflectivity suggests that the film is highly hydrated. As the pressure increases above ~ 5 mN/m, the film becomes incompressible and a second but inhomogeneous layer is formed on the first one. This second layer does not contribute to the 2D Bragg reflection observed from the monolayer implying that it is highly disordered lacking short-range order.

Acknowledgment. We thank D. S. Robinson for his help at the 6ID-B beamline, and to J. McManus for his help in data acquisition of the isotherms. The Midwest Universities Collaborative Access Team (MUCAT) sector at the APS is supported by the U.S. Department of Energy, Basic Energy Sciences, Office of Science, through the Ames Laboratory under Contract No. W-7405-Eng-82. Use of the Advanced Photon Source was supported by the U.S. Department of Energy, Basic Energy Sciences, Office of Science, under Contract No. W-31-109-Eng-38.

References and Notes

- (1) Coronado, E.; Delhaes, P.; Gatteschi, D.; Miller, J. S., Eds. *Molecular magnetism: From Molecular Assemblies to Devices*; Kluwer Academic Publishers: Norwell, MA, 1996 and references therein.
- (2) *Quantum Tunneling of the Magnetization*; Gunther, L., Barbara, B., Eds.; NATO ASI Series E 301 Kluwer: Dordrecht, 1995.
- (3) Atkinson, I. M.; Benelli, C.; Murrie, M.; Parsons, S.; Winpenny R. E. P. *Chem. Commun.* **1999**, 285–286.
- (4) Miller, L. L. Unpublished.
- (5) Clemente-León, M.; Mingotaud, C.; Agricole, B.; Gómez-García, C. J.; Coronado, E.; Delhaes, P.; *Angew. Chem., Int. Ed. Engl.* **1997**, *36*, 1114–1116.
- (6) Clemente-León, M.; Soyer, H.; Coronado, E.; Mingotaud, C.; Gómez-García, C. J.; Delhaes, P.; *Angew. Chem., Int. Ed.* **1998**, *37*, 2842–2845.
- (7) Fukuto, M.; Penanen, K.; Heilmann, R. K.; Pershan, P.; Vaknin, D. *J. Chem. Phys.* **1997**, *107*, 5531–5546.
- (8) Parratt, L. G. *Phys. Rev.* **1954**, *59*, 359–369.
- (9) Vaknin, D.; Wang, J. Y.; Uphaus, R. A. *Langmuir* **1995**, *11*, 1435–1438.
- (10) Vineyard, G. *Phys. Rev. B* **1982**, *26*, 4146–4159.
- (11) Vaknin, D. <http://xxx.lanl.gov/ps/cond-mat/0101142>, **2001**, 1–56.